U. S. NAVAL ORDNANCE TEST STATION

W. W. Hollister, Capt., USN
Commander

Wm. B. McLean, Ph.D.
Technical Director

NOTS 1939 NAVORD REPORT 5842

HYDRODYNAMIC DRAG OF TORPEDOES

By

J. D. Brooks
and
T. G. Lang

Underwater Ordnance Department

This report, published by the Underwater Ordnance Department, is the approved version of 807/MS-99. It consists of cover, 29 leaves, and abstract cards. From the original printing of 125 copies, this document is

Copy No 101

China Lake, California

18 February 1958

FOREWORD

This report presents, first, a method for selecting a torpedo body shape that will have minimum drag and, second, a modification of the method for estimating the drag of existing torpedoes. It is intended for use in preliminary design and in analysis.

The work was done at the U. S. Naval Ordnance Test Station from August 1956 to September 1957 under Bureau of Ordnance Task Assignment NO-404-664/41001/01054. The report was reviewed for technical adequacy by H. T. Yerby and J. W. Hoyt of this Station.

D. J. WILCOX, Head
Underwater Ordnance
Department

Released under
the authority of:

WM. B. McLEAN
Technical Director

ABSTRACT

The experimental drag data from a large number of tests of bodies of revolution, with and without appendages, were analyzed. Semiempirical relations were developed and then extended theoretically. The results in graph form show the variation of drag coefficient with tail shape, nose shape, and cylinder-section length for stable torpedo configurations having constant volume and velocity. From these data, methods were developed for obtaining an optimum configuration for any given set of design specifications. In addition, a method is presented for quick calculation of the drag of any torpedo with arbitrary fin size, roughness, holes, tail cutoff, volume, and velocity.

CONTENTS

INTRODUCTION

Modern undersea warfare requires torpedoes that combine high speed, long range, and precise maneuverability in a small and compact vehicle. To achieve this, not only the internal components but also the external hydrodynamic shape must be optimized. Where some latitude exists in the design specifications, it is desirable to select a body form and stabilizing fins having the least drag for a given volume. The methods presented here enable the designer to estimate the drag of a torpedo configuration quickly and accurately and to select the optimum shape within the given specifications.

Theoretical methods employing boundary-layer theory are available for estimating the drag of a submerged body, but in general the computation required is prohibitive. Much experimental data have been obtained on the drag of underwater body shapes, but careful analysis of this information shows considerable scatter. The most commonly used method for quickly estimating the drag of a torpedo consists, first, of calculation for skin friction of the body and fins by using the turbulent flat-plate drag coefficient, then the addition of a certain percentage for body form drag and another percentage for interference effects and fin-form drag.

Refinements that allow for differences in nose shape, tail-cone shape, cylinder-section length, and fin size, and for variations of surface roughness and number of holes or protuberances are seldom included in the calculations.

A method is presented here for estimating torpedo drag as a function of the effects of these differences and variations. The accompanying graphs, which show these effects qualitatively, are intended for use in a quick calculation of an optimum design. Additional graphs are included for use in estimating the drag of the optimum design. Then, a modified procedure is described that may be used for estimating the drag of any existing torpedo.

The analysis used in preparing this report is both empirical and theoretical in nature. An attempt is made to correlate the known experimental data on streamlined body shapes with theory and additional experimental data on the effects of body-shape variations and fin drag.

DRAG OF STREAMLINED BODIES

A large number of experimental drag tests were conducted on streamlined bodies of revolution at zero angle of attack in incompressible flow. Since there is much scatter and conflict among the test data, the first step must be an attempt at correlation before the torpedo drag can be analyzed. This torpedo drag is composed of frictional drag and form drag. It is a well-known

result of fluid mechanics that the drag of any body in a nonviscous fluid is zero, even though there exists a pressure distribution over the body. Friction drag is the sum of the viscous shears in the boundary layer, and form drag is the result of the difference in integrated pressure over the nose and tail sections caused by the finite thickness of the boundary layer streaming off to infinity in the wake.

Most torpedoes operate at speeds sufficiently high that the boundary layer is fully turbulent. Therefore, this report is concerned only with those submerged body shapes over which the flow is fully turbulent and where no separation occurs, except possibly at the tail cone. Unfortunately, many water- and wind-tunnel tests have been conducted at low Reynolds numbers where some laminar flow is likely to occur at the nose. This situation is clearly illustrated in Fig. 1 (Fig. 2 from Ref. 1) showing the results of drag measurements taken on a single model in a variable-density wind tunnel where the pressure is varied. It can be seen that in the transition region $2 \times 10^6 < R_\ell < 2 \times 10^7$ there is considerable scatter in the drag measurements, indicating the presence of laminar flow, whereas above $R_\ell = 2 \times 10^7$ there is little scatter, indicating fully turbulent flow. Sometimes, in tunnel tests, transition to turbulent flow is artificially stimulated by roughening the nose section, but the results of such practice on models have not always agreed with those of full-scale models.

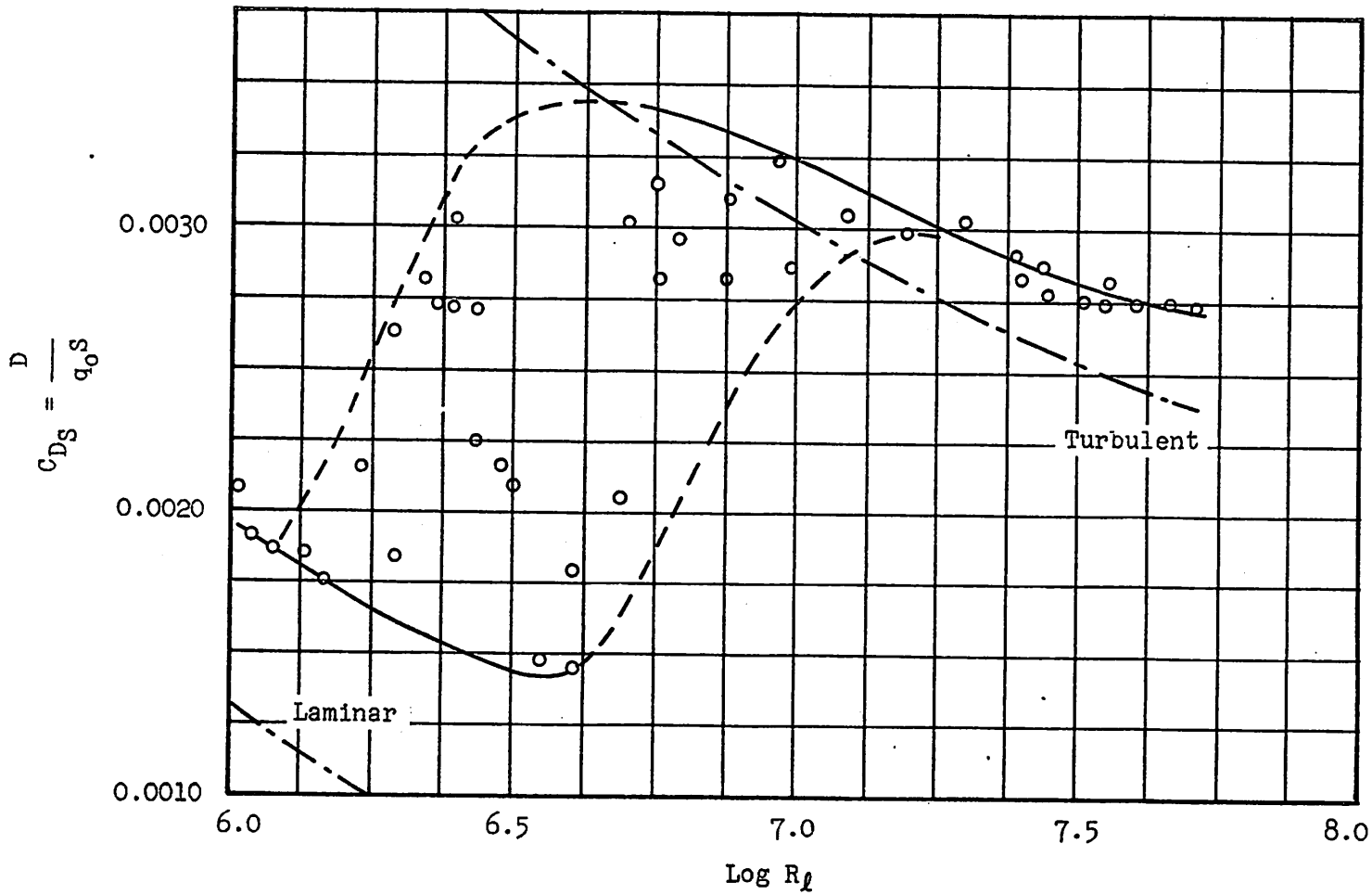

FIG. 1. Variation of Drag Coefficient With Reynolds Number and Tunnel Pressure for a Given Streamlined Body.

The basic drag data used in this report are results of tests on streamlined bodies shown in Fig. 2 where the skin friction in each instance, including the overvelocity effect, has been adjusted to a standard Reynolds number of 2×10^7, with the form drag kept constant. It is believed that the wide scatter in these data is due mainly to tests in the transition region of Reynolds number and to differences in test equipment and technique, test fluid nature and turbulence, model roughness, and strut interference. A mean line has been drawn through those points which are regarded as most reliable. The criteria used in judging the test validity are shown in Table 1.

The tests at the David Taylor Model Basin (DTMB) are considered the most reliable and were conducted on bodies having fineness ratios of 4 and larger. In the range of fineness ratios less than 4, a theoretical drag estimate was obtained using Ref. 5, which agreed with some data taken by the National Advisory Committee for Aeronautics (NACA) at a low Reynolds number; therefore, the mean line was drawn through these points.

It is noted that the drag data considered most reliable are obtained from a water basin. This is in accord with the statement of Hoerner[1] that transition from laminar to turbulent flow occurs, for some unknown reason, at a lower Reynolds number in water than in air.

---

[1] Hoerner, S. F. Fluid-Dynamic Drag. To be published.

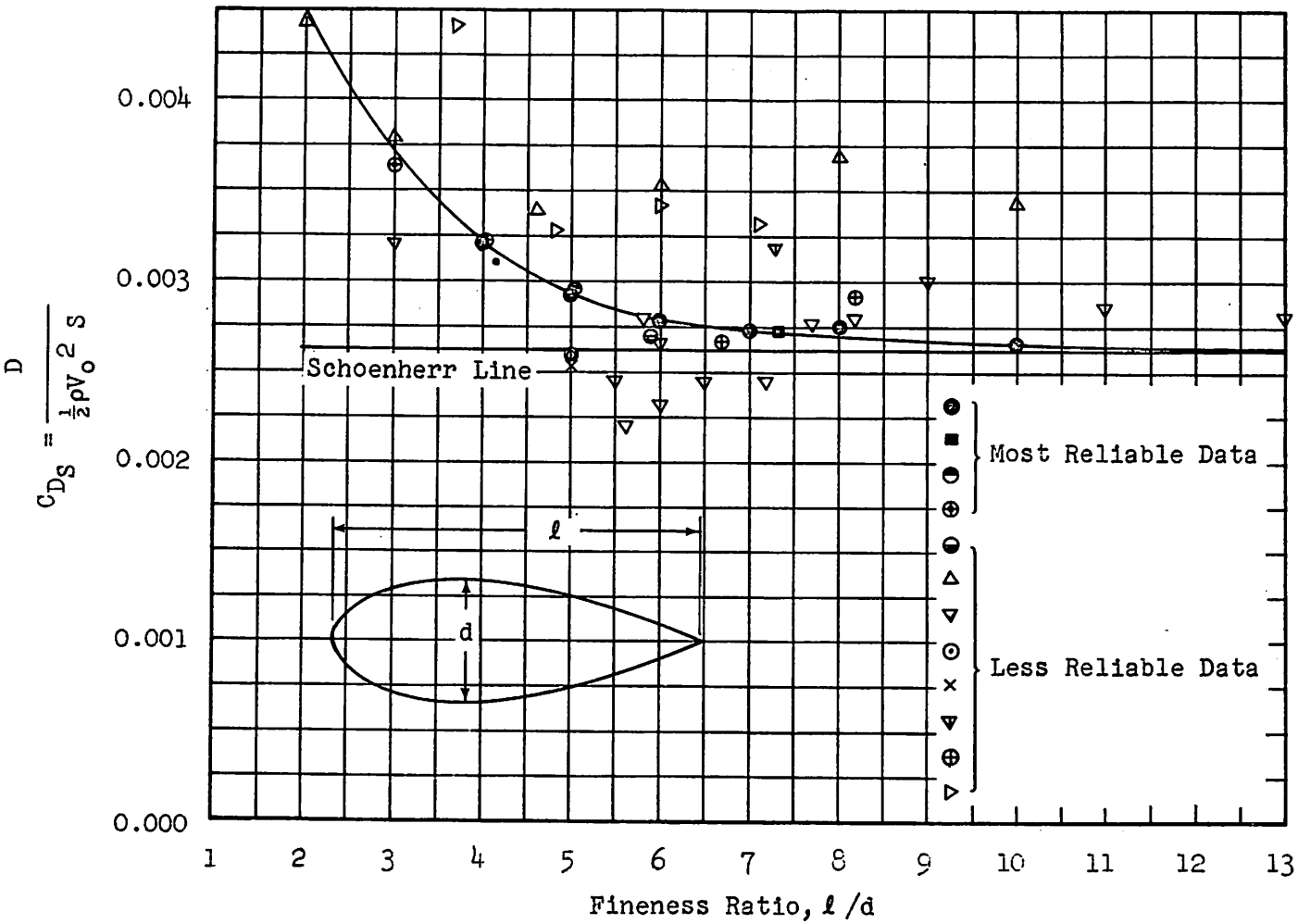

FIG. 2. Drag Coefficient Versus Fineness Ratio for Streamlined Bodies $R_\ell = 2 \times 10^7$.

TABLE 1. Basic Drag Data

The first four symbols are the more reliable data; the remainder are less reliable.

Symbol	Reference	Test R_ℓ	Scatter of Data	Turbulence Stimulation	Type of Tunnel	Support Correction
○	DTMB, Ref. 2	2×10^7	Small	Yes	Water	Small
□	DTMB, Ref. 3	2×10^7	Small	Yes	Water	Small
◇	DTMB, Ref. 4	2×10^7	Small	Yes	Water	Small
⊕	ARC, Ref. 5	.....	Theoretical points; valid if no separation			
◎	NACA, Ref. 6	2×10^7	Medium	No	Air (Variable Density)	Medium
△	NACA, Ref. 7	7×10^5 to 3.6×10^6	Large	No	Air	Large
▽	ZWB, Ref. 8	5.4×10^6	Large	No	Air	Large
◎	SIT, Ref. 9	2.7×10^6	.....	Yes	Water	Small
×	NACA, Ref. 10	2.2×10^7	.....	No	Air	Small
▽	SIT, Ref. 11	7×10^6	Large	Yes	Water	Small
⊕	NPL, Ref. 12	4.8×10^6	Large	No	Air (Variable Density)	Medium
▷	NACA, Ref. 13	2×10^7	Large	No	Air (Variable Density)	Medium

The drag measurements included in Fig. 2 are all obtained from tests of streamlined bodies having similar shapes. Reference 2 shows that small changes in the position of maximum thickness and in prismatic coefficient have only a small effect on drag. Consequently, the mean line for drag as a function of fineness ratio in Fig. 2 is considered valid for streamlined bodies in fully turbulent flow when the prismatic coefficient is approximately 0.6 and the position of maximum thickness is approximately 0.4ℓ from the nose.

A graph of the skin-friction coefficient based on body surface area is plotted in Fig. 3 as a function of Reynolds number. The coefficient was obtained from the well-known Schoenherr turbulent skin-friction drag of a flat plate. It was corrected for overvelocity effects by using the results of theoretical calculations from Ref. 5. Figure 4 shows the form or residual drag coefficient based on body-surface area C_r, obtained by subtracting the drag coefficients shown in Fig. 3 from those in Fig. 2.

DRAG OF GENERAL BODY SHAPES

The effect on drag of changes in body shape and of the addition of appendages can be explained by considering the same physical concept mentioned on page 3--that of a viscous boundary layer on which is superimposed the ideal fluid pressure distribution. It can be seen that an increase in length of the cylindrical midsection can cause

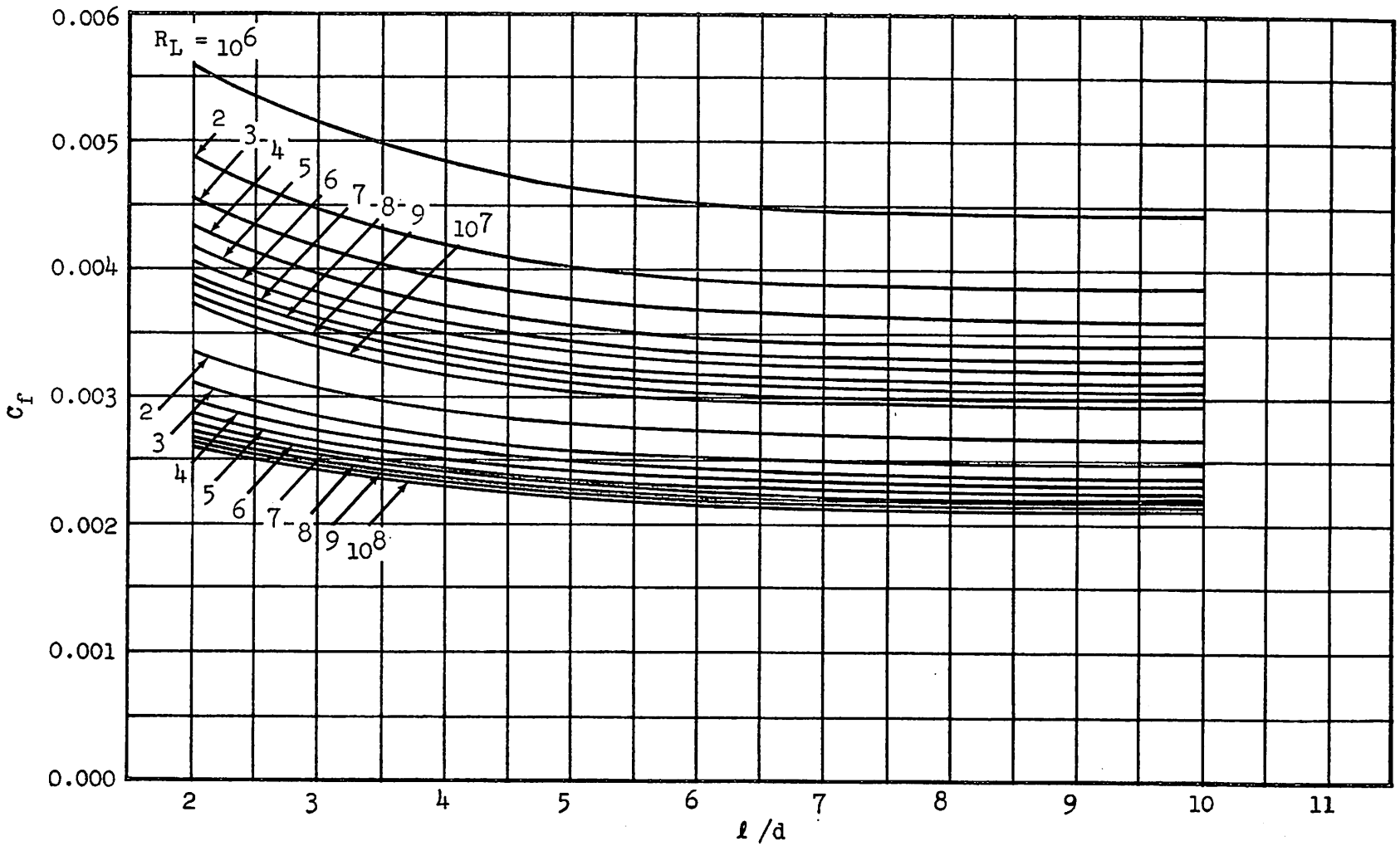

FIG. 3. Turbulent-Skin Friction Coefficients for Streamlined Bodies of Revolution $C_f = \dfrac{D_f}{\frac{1}{2}\rho V_o^2 S}$

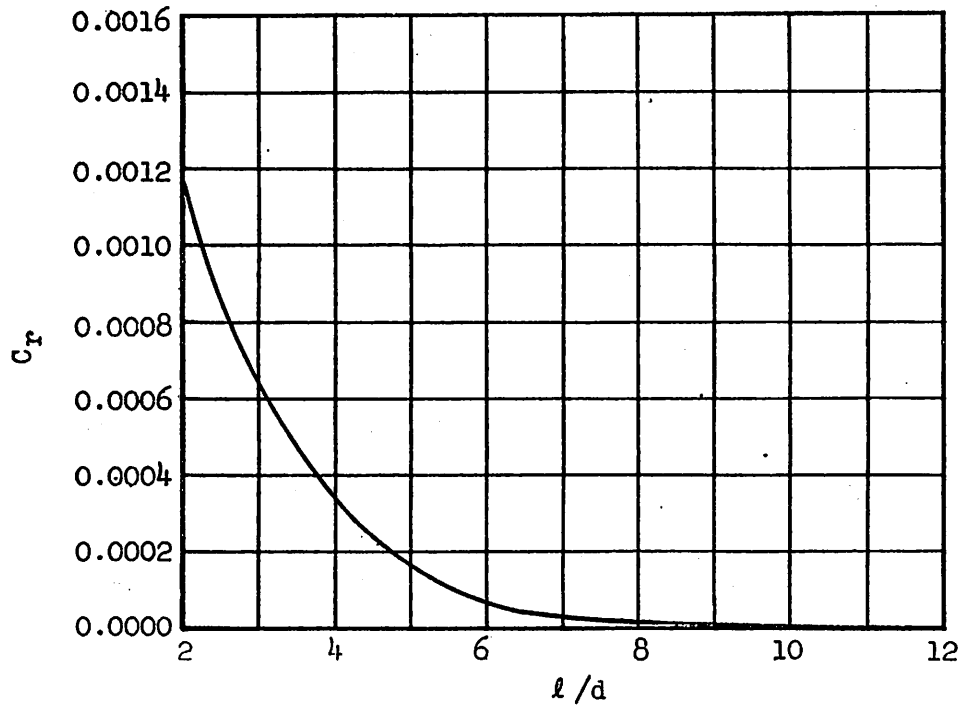

FIG. 4. Pressure Drag Coefficient C_r for Streamlined Bodies $C_r = C_{D_S} - C_f = \dfrac{\text{Pressure Drag}}{q_o S}$.

additional friction drag because of the added shear in the boundary layer, and additional form drag because of the effect on the thickness of the boundary layer at the tail. Also, any change of shape that changes the pressure distribution on the body, such as a gross change in nose shape, cut-off tail cone, or stabilizing fins, can cause a corresponding change in form drag; and any change in surface condition or roughness that influences the shear in the boundary layer can cause added friction drag. These effects will be investigated in the following sections.

CYLINDRICAL SECTION

The effect on drag of the addition of cylindrical midsections to a torpedo body has been tested at a number of facilities. The results of these tests are inconclusive, since they were made at different Reynolds numbers and with high strut-drag corrections. An analysis of data similar to that made for the streamlined body drag shows that the best data obtained on torpedo bodies with varying cylindrical-section lengths were taken at DTMB (Ref. 14). A theoretical method is described in Ref. 15 for estimating the drag of a body of revolution. This method was modified by making simplifying assumptions (as described in Appendix A) and then used to calculate the added form drag caused by the increased boundary-layer thickness over the cylindrical section. The results are combined with the tail-cone form drag of streamlined bodies and shown in Fig. 5 as the total drag coefficient of torpedo bodies based on body volume as a function of tail-cone shape and cylindrical-section length. Good agreement was obtained with the experimental results of Ref. 14. The theoretical cylindrical-section drag was estimated for a particular range of Reynolds numbers as described in Appendix A, but it is believed that the increase in form drag attributable to the cylindrical section will remain reasonably independent of Reynolds number in the range of torpedo applications.

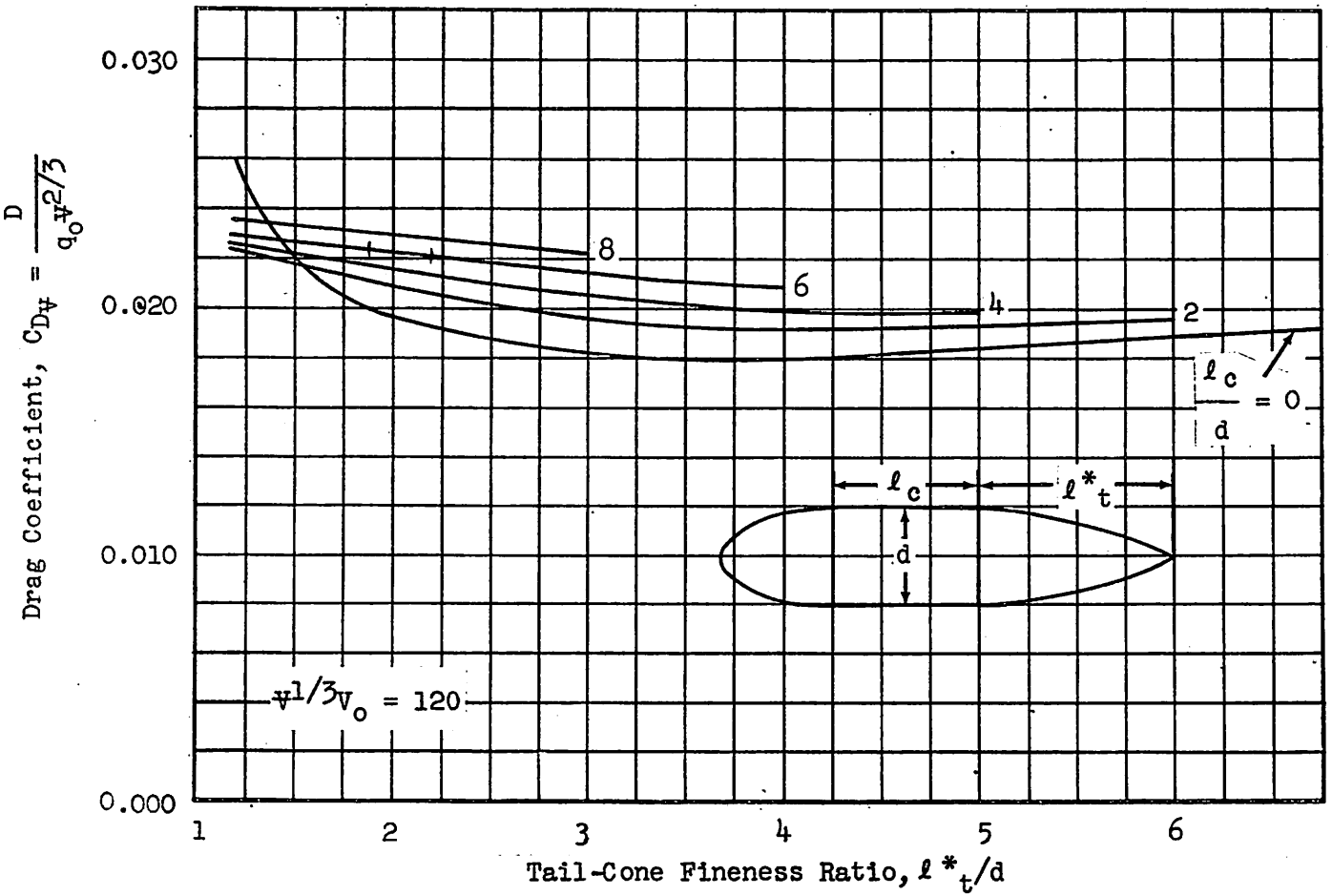

FIG. 5. Drag Coefficient Based on Volume for Streamlined Bodies With Cylindrical Sections. Parent tail-cone shape, DTMB Series No. 58. Fully turbulent flow.

NOSE SHAPE

A number of experimental tests have been made on torpedo models with different nose sections. Although some differences were noticed, the general conclusion is that the form drag of a torpedo body is independent of the nose shape when no separation occurs on the nose section and when the boundary layer is fully turbulent. This finding also agrees with the theory that the form drag of a nose section attached to a very long body is zero. Therefore, it can be assumed that, within the practical range of torpedo fineness ratios, the pressure distribution on the nose has negligible effect on the pressure distribution on the tail. It is possible, however, that for very short bodies (small fineness ratios), the form drag will be influenced by the nose shape. Consequently, nose sections now in use can be considered to have purely frictional drag and the total form drag considered a function of the tail-cone shape and the boundary-layer thickness at the tail cone.

The curves of drag coefficient for a family of torpedoes are shown in Fig. 5. This family has over-all fineness ratios which are 1.67 that of each particular tail-cone fineness ratio, since the tail-cone length is 0.6 the length of the parent streamlined body. These same curves can be used to estimate the drag of a torpedo having any nose shape, if separation does not occur, by including a nose-shape correction factor. It is assumed that two

noses having the same volume also have approximately the same skin-friction drag. For example, on a blunt nose the effect of over-velocity is to increase the nose drag, but this is in turn reduced by the decreased surface area. Figure 6 shows the nose-shape correction factor that must be used in applying Fig. 5 for estimating torpedo drag. This factor is the effective change that must be made to the cylindrical-section length ordinarily used so that the volume of the actual torpedo nose plus the volume of the cylindrical-length correction is equal to the volume of the basic streamlined nose section used in Fig. 5. Consequently, to use Fig. 5, the fineness ratio of the torpedo cylindrical section must be changed by the amount shown in Fig. 6.

CUT-OFF TAIL CONE

Frequently, the tail cone of a torpedo is truncated. The added drag of this bluff base is a function of the boundary-layer thickness and the diameter of the cut-off. The drag coefficient for the truncated tail cone is expressed in Ref. 16 as

$$C_{D_{A_c}} = \frac{0.029}{\sqrt{C_f \frac{S_{wet}}{A}}} \left(\frac{d_B}{d}\right)^3 \quad (1)$$

For standard torpedoes, the expression under the radical can be approximated as follows:

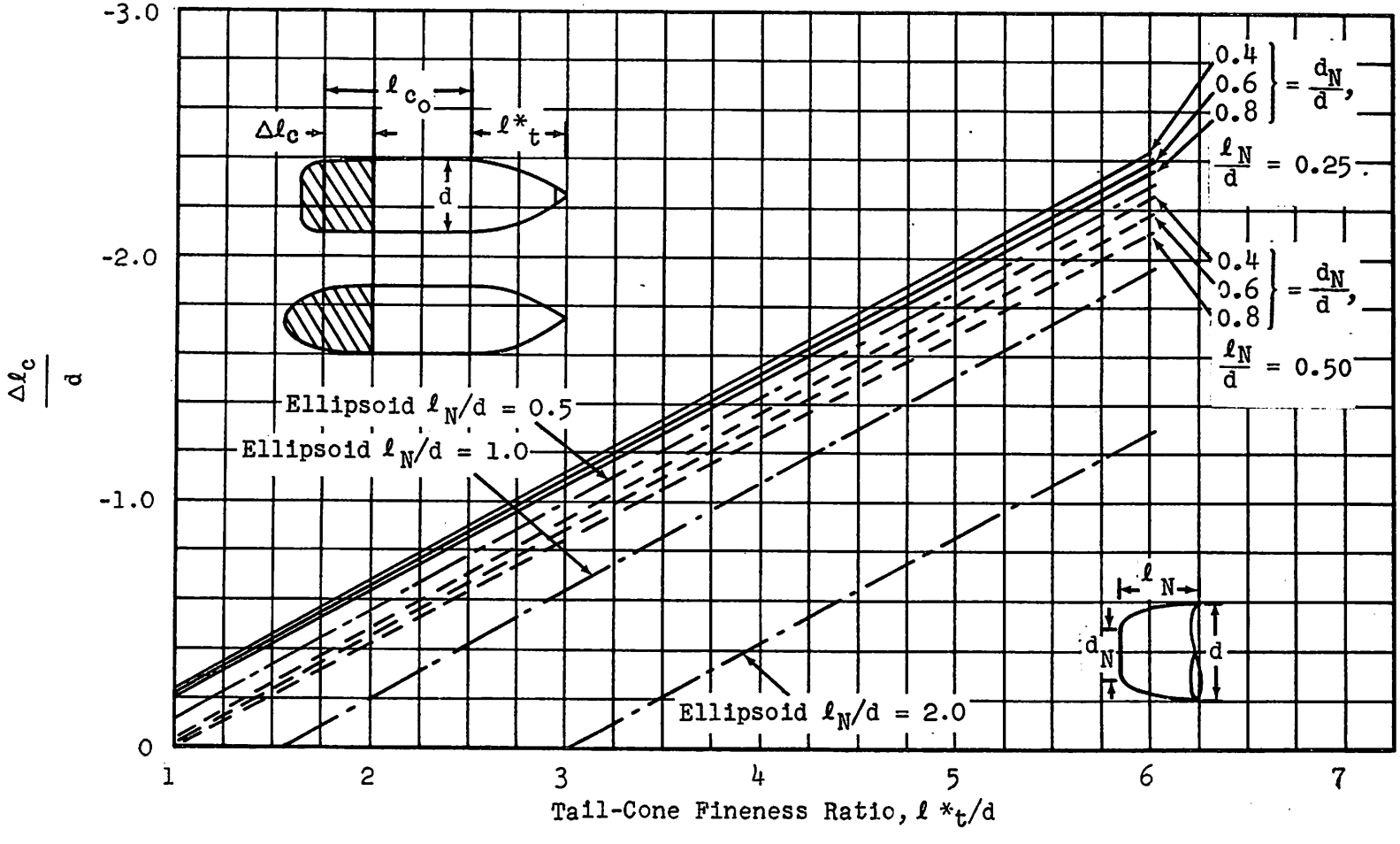

FIG. 6. Nose Shape Correction Factor.

$$C_f \cong 0.003$$

where $$R_\ell \cong 10^7$$

$$S_{wet} \cong 0.8\pi \frac{\ell^*}{d} d^2$$

and $$A = \frac{\pi}{4} d^2$$

therefore

(2) $$C_{D_{A_c}} \cong \frac{0.29}{\sqrt{\ell^*/d}} \left(\frac{d_B}{d}\right)^3$$

This function is graphed in Fig. 7 for use in estimating the drag of torpedoes which have large cut-off diameters. For the normal range of torpedo bodies having cut-off diameters less than one-fourth the maximum diameter, Fig. 7 shows the drag increase to be less than 2 percent and therefore negligible. Thus the drag of torpedoes with small cut-off diameters may be estimated by assuming that the tail cone is streamlined and by measuring a length ℓ_t^* out to the projected tip. When very short tail cones are used and separation occurs, the drag caused by truncation is zero if the cut-off is back of the separation point.

SURFACE ROUGHNESS

The drag coefficient correction for roughness, based on body surface area, can be obtained from Fig. 8 which was drawn from data reported in Ref. 6 and modified for torpedo use in Ref. 17. This correction factor can be based on cross-section area of the torpedo

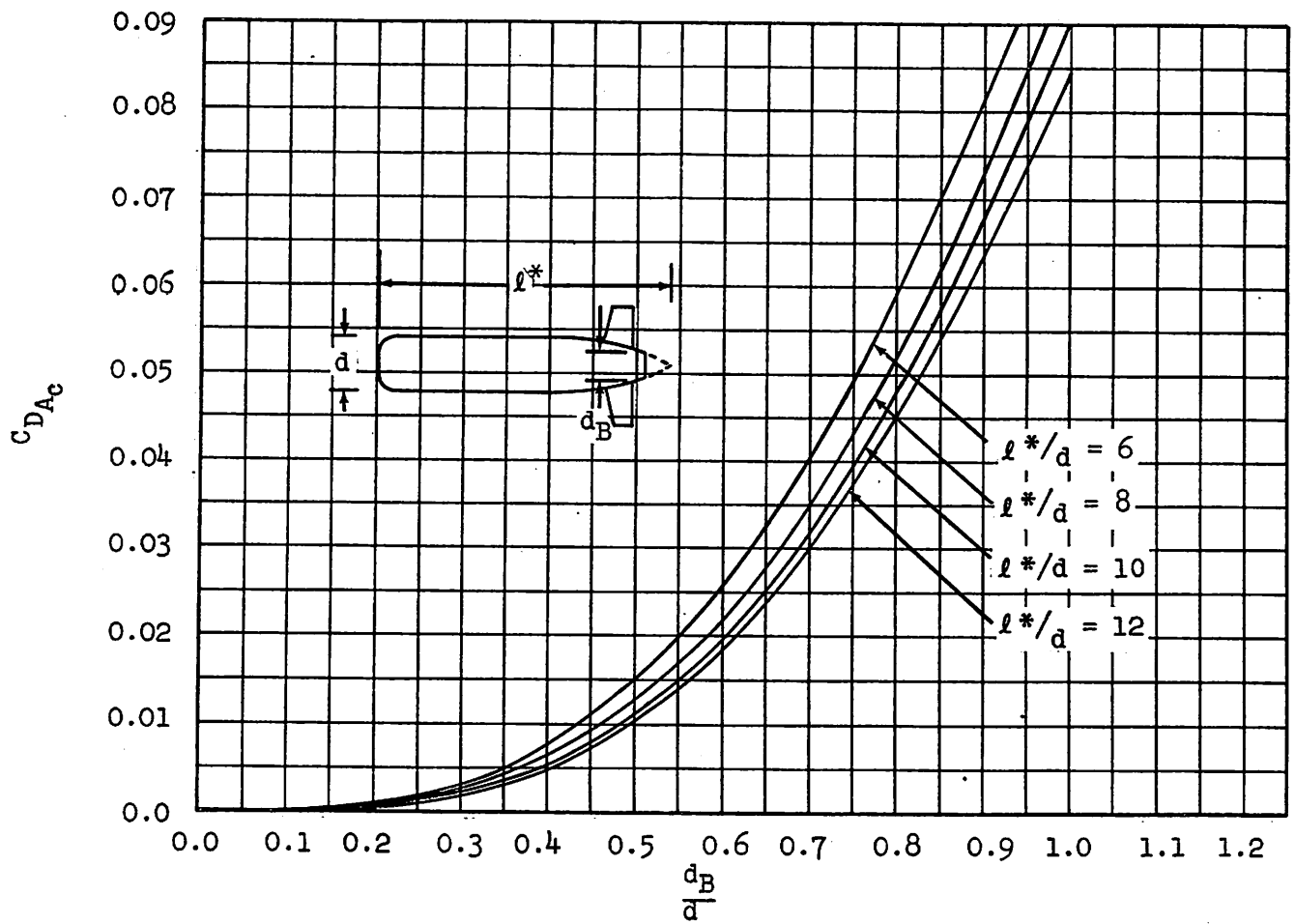

FIG. 7. Added Drag Caused by Truncated Tail Cone. Wetted surface coefficient $\cong 0.8$, $R_\ell \cong 10^7$.

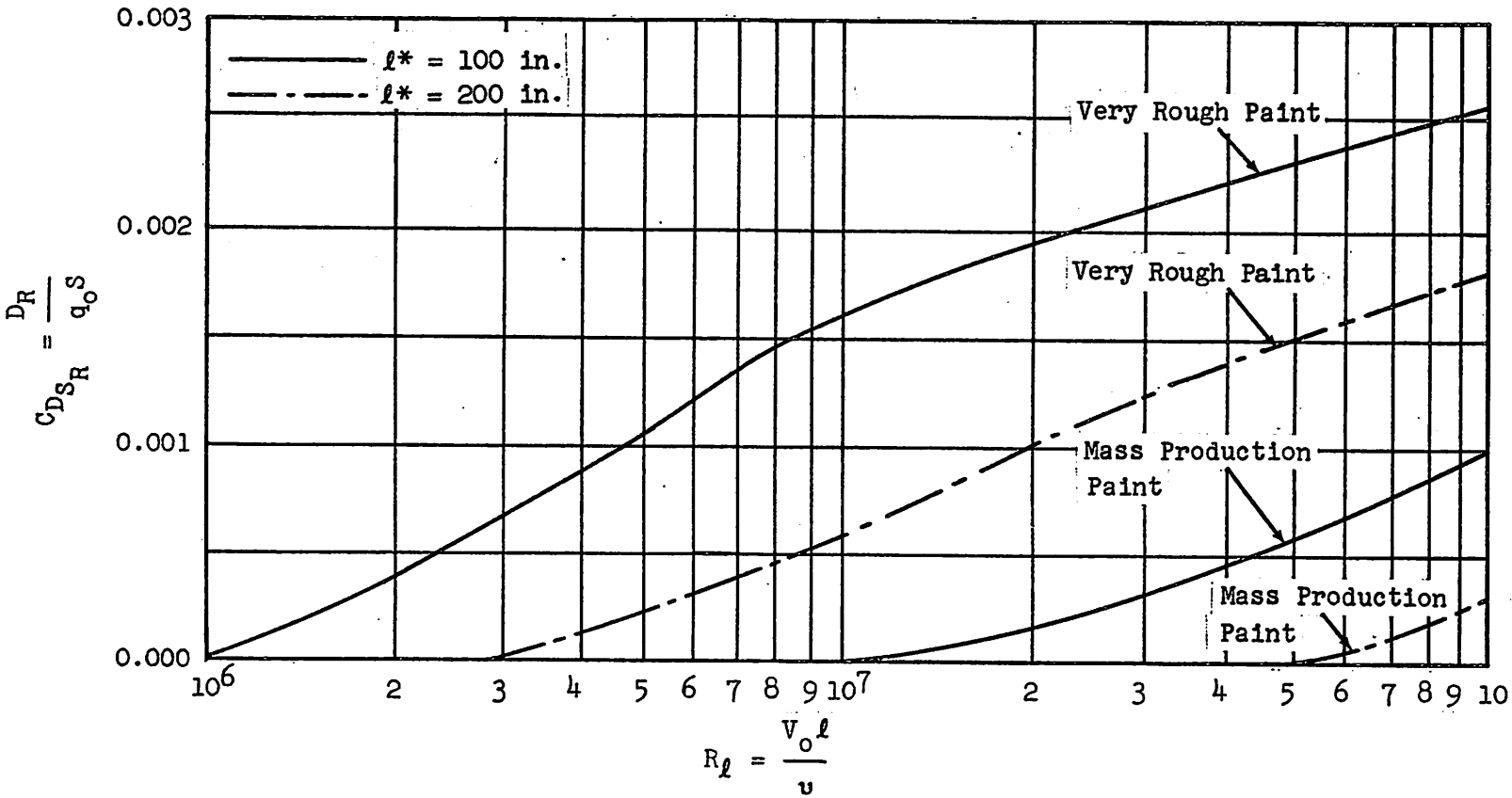

FIG. 8. Roughness Coefficient $C_{D_{S_R}}$ as a Function of Reynolds Number, Torpedo Length, and Surface Finish.

rather than surface area if the assumption is made that the body surface area is

$$S \cong 0.8\pi \ell^* d$$

Then to a close approximation,

$$(3) \qquad C_{D_{A_R}} \cong 0.31\, C_{D_{S_R}}\, d/\ell^*$$

The correction for very smooth surfaces is zero.

The added drag of holes and protuberances can be estimated by using methods given by Hoerner in Ref. 16.

DRAG OF STABILIZING FINS

Basically, the method used for calculation of fin drag is presented by Hoerner (Ref. 16). The calculation explained in detail in Appendix B of this report was done according to Hoerner's method and by the use of a correction factor computed from empirical data. A simplified explanation is given below.

The fin drag based upon the wetted fin-surface area for tail fins located along the rear portion of the tail cone is

$$(4) \quad C_{D_{S_f}} = \frac{\text{Fin drag}}{q_o S_f} = 0.93\, C_{f_{fin}}\left(1.135 + 2\frac{t}{c}\right) + \frac{t}{b-a}\left(0.16\frac{t}{c} + 0.017\right)$$

$$-0.00024\frac{c}{b-a} + 0.00093\left(9.5 - \frac{\ell^*}{d}\right)$$

The first three terms represent the skin friction corrected for overvelocity plus body-fin pressure interference effects, and the last term is an empirical correction for boundary-layer

interference between the body and fins, where ℓ^*/d is the fineness ratio of the body. This last term was obtained from experimental drag data for 12 different airships and torpedoes which were tested with and without fins. The term represents the difference between the experimental fin drag and that portion of the theoretical drag of the fins that can be calculated. The scatter in the data shown in Fig. 9 is significant. These data, however, represent the best that is currently available. More tests should be conducted in the future to reduce this scatter, since this term is important in selecting an optimum body shape for minimum drag.

If the fins are attached to the body at positions other than the tail cone, or if cruciform fins of radical design or a shroud ring are used for stability, a modification of the procedure shown in Appendix B and Ref. 16 can be used for estimating the drag. All the data seem to indicate, however, that cruciform fins provide the most stability for the least drag.

OPTIMUM BODY SHAPE

Much interest has been shown by a number of investigators in determining the optimum body shape for a torpedo. Reference 2 shows that the minimum drag per unit volume for a streamlined body occurs at a body fineness ratio of 6.5, which corresponds to a tail fineness ratio of 3.9. Reference 14 explains the effect of the variation of cylindrical midsection length on the drag of a single

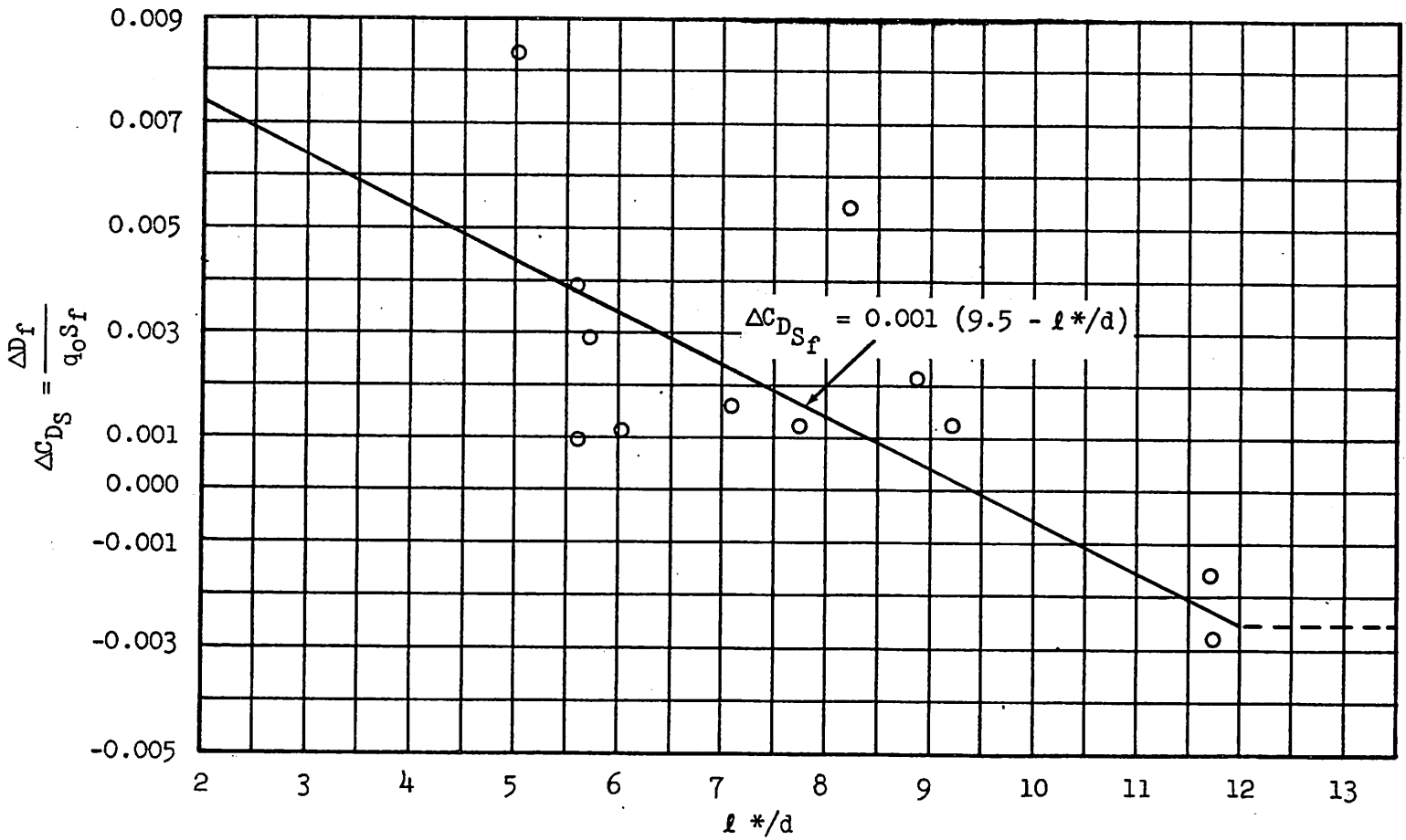

FIG. 9. Drag Increment From Boundary-Layer Interference Drag.

parent form. However, there are no systematic series of tests to show the combined effect of nose shape, tail-fin size, tail-cone fineness ratio, and cylindrical midsection length, probably because the number of different models and tests required would be prohibitive. Nevertheless, it is possible to approximate, theoretically, this combined effect by applying the method described in this report to different torpedo configurations, each configuration representing a different body shape to which is appended the proper-size fin to achieve constant torpedo stability. Drag data for a series of fully appended torpedoes can thus be achieved.

In order to compare the effect of differences in body shape on drag, torpedo volume and velocity were held constant. To accomplish this it was assumed that $\forall^{1/3} V_o$ = a constant. To make the study more general, the drag can be expressed in coefficient form where $C_{D_\forall} = \frac{D}{\forall^{2/3} q_o}$. This drag coefficient will be constant for all geometrically similar torpedoes which operate at the same Reynolds number $R_\ell = \frac{\ell V_o}{\upsilon}$. Since ℓ is proportional to $\forall^{1/3}$, R_ℓ is proportional to $\forall^{1/3} V_o$. Therefore, $C_{D_\forall}$ is a measure of the drag per unit volume for a series of torpedoes where $\forall^{1/3} V_o$ is a constant. An arbitrary value for $\forall^{1/3} V_o$ of 120 was selected, which corresponds to families of torpedoes having a volume of 20 cu ft running at 44 fps, a volume of 10 cu ft running at 56 fps, or a volume of 5 cu ft running at 70 fps.

Consequently, the Reynolds number of the torpedo bodies satisfying these conditions varies, depending upon body fineness ratio. It is assumed that the flow is fully turbulent and that no flow separation exists over the nose. Although the skin friction will change when other sizes or velocities are considered, it is believed that the optimum design point and qualitative differences between shapes will not noticeably vary. The results of the computations are shown in Fig. 5 and 10 where the drag coefficient based upon body volume is presented for bare bodies and fully appended bodies, respectively, as a function of tail-cone fineness ratio and cylindrical-section length, where $\forall^{1/3} V_o = 120$. The nose correction factor is obtained from Fig. 6. A study of Fig. 5 and 10 shows that the drag per unit volume of a bare torpedo body is minimized when the body is fully streamlined and has a tail-cone fineness ratio of 3.9, which corresponds to a body fineness ratio of 6.5. Replacement of the streamlined nose with a well-designed blunt nose may slightly decrease the drag if the flow is fully turbulent in both situations. The minimum drag per unit volume of fully appended torpedoes occurs when the tail-cone fineness ratio is 6 or greater. When the tail-cone fineness ratio is smaller, minimum drag occurs when the cylindrical-section length is equal to or greater than six torpedo diameters. The addition of a blunt nose in this instance increases the drag slightly for low body fineness ratios and has no effect for the higher body fineness ratios. Consequently, it is seen that the minimum drag per unit volume for

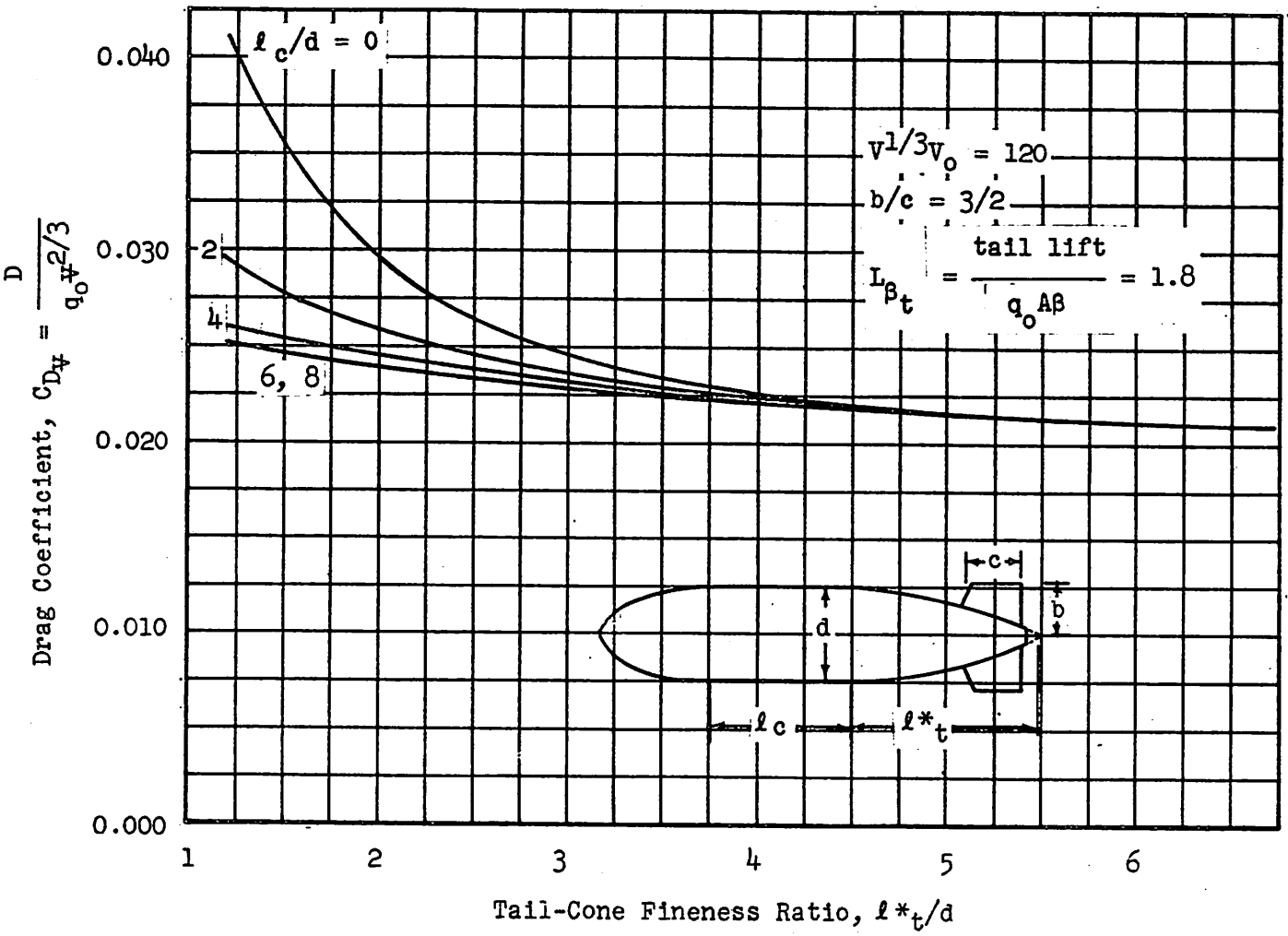

FIG. 10. Drag Coefficient Based on Volume for Torpedoes With Stabilizing Fins. Parent tail-cone shape, DTMB Series No. 58. Fully turbulent flow.

different body shapes depends on the presence or absence of stabilizing fins. The optimum shape, however, is not critical, so that a small variation in body shape is acceptable. Figures 5 and 10 show the effect of large body-shape variations on the drag per unit volume.

DRAG OF THE FULLY APPENDED TORPEDO

The drag coefficient of a fully appended torpedo can be estimated by one of three methods outlined below. In general, these methods are not valid for estimating the drag on submarines because of the effect on form drag of widely divergent Reynolds numbers, and the presence of various nonstreamlined protuberances and appendages, for example, conning tower, bow planes, etc.

Method A: Drag Coefficients for Standard Torpedoes[2] When $\forall^{1/3} V_o \approx 120$. Method A is valid for selecting the optimum body shape and estimating the drag coefficients of geometrically similar torpedoes, with fin size and stability similar to that defined in Appendix B, for which the $\forall^{1/3} V_o$ constant is close to 120. It is first necessary to obtain the fineness ratio of the tail cone (measured to extended tip) ℓ^*_t/d, cylindrical section $\ell c_o/d$, nose ℓ_n/d,

[2] A purely arbitrary term designating torpedoes of the geometric similarity, stability, and surface condition selected for this study. Similarly, nonstandard torpedoes have characteristics differing greatly from those selected for this study.

and nose flat d_n/d. The nose correction factor is then obtained from Fig. 6, and the drag coefficient based on volume from Fig. 10. For convenience in application, the drag coefficient based on body cross-sectional area is shown in Fig. 11.

Method B: Drag Coefficients for Standard Torpedoes of Any Volume or Velocity. Method B is valid for selecting optimum body shape and estimating the drag coefficients of torpedoes in the same family as those considered in Method A (fin size and stability similar to that defined in Appendix B) but for which the $\forall^{1/3} V_o$ constant differs in a marked degree from 120. Again, it is necessary to obtain the fineness ratios of the tail cone, cylindrical section, nose, and nose flat. The Reynolds number is $R_\ell = \frac{V_o \ell}{\upsilon}$ where $\upsilon = 1.3 \times 10^{-5}$ for sea water at 60°F. The drag coefficient based on cross-sectional area is found from Fig. 12 after the nose correction factor (Fig. 6) is applied.

Method C: Drag Coefficients for Nonstandard Torpedoes. Method C is valid for selecting optimum body shape and estimating drag coefficients for torpedoes whose velocity, displacement, and fin size vary widely from the series of torpedoes considered in this study. To correct the C_{D_A} found in Method B for the effect of roughness, protuberances, and fin size, the fin dimensions a, b, c, and t (Fig. 13) must be obtained. The roughness and parasite drag coefficients $C_{D_{S_R}}$ and $C_{D_{A_{parasite}}}$ are obtained from Fig. 8 and Ref. 16, respectively. The drag of a blunt tail cone is

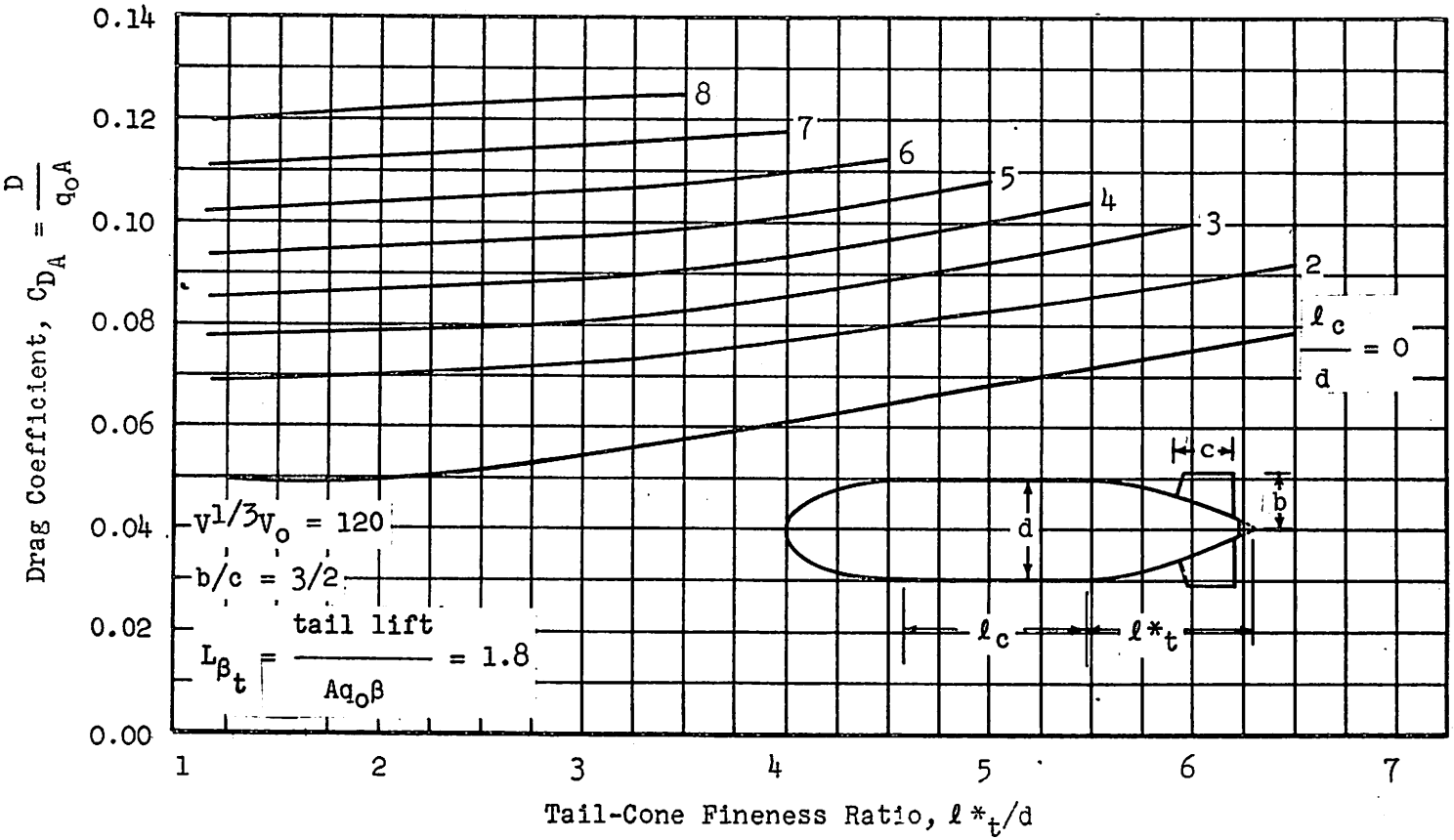

FIG. 11. Drag Coefficient Based on Cross-Section Area for Torpedoes With Stabilizing Fins. Parent tail-cone shape, DTMB Series No. 58. Fully turbulent flow.

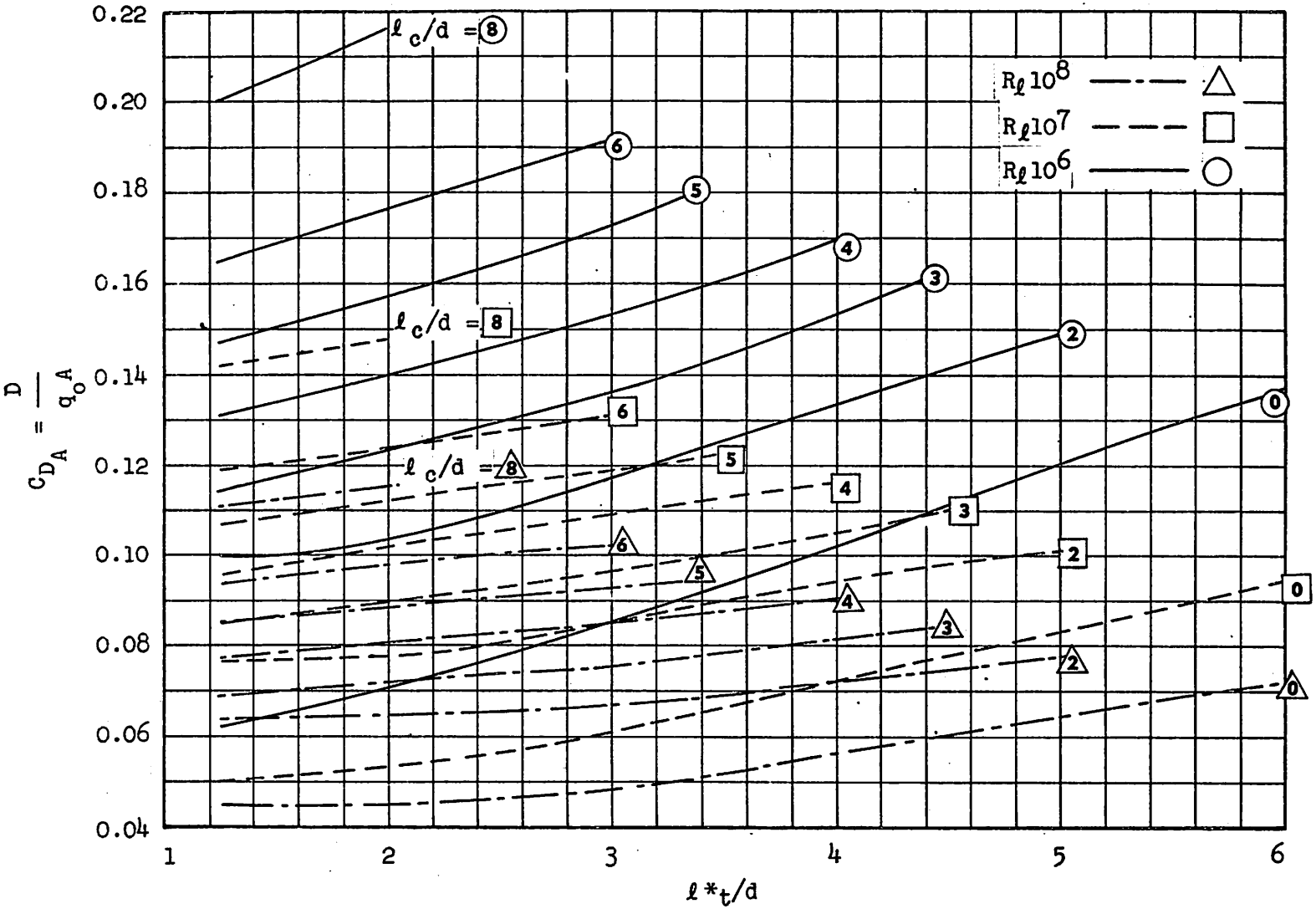

FIG. 12. Drag Coefficient Based on Cross-Section Area for Fully Appended Torpedoes.

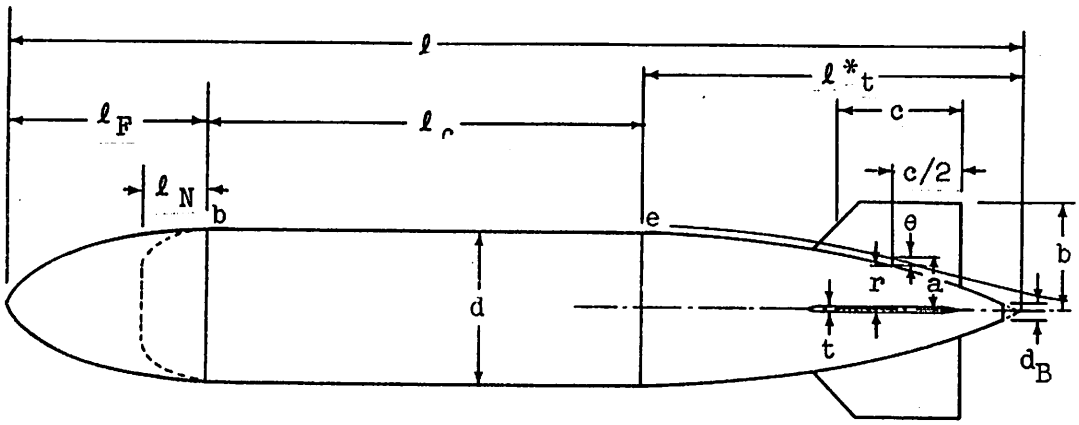

FIG. 13. Parameters of a Typical Torpedo.

important if the cut-off diameter is greater than one fourth the torpedo diameter, and it is obtained from Fig. 7. The fin drag is obtained from Appendix B, and for convenience of application is used as a correction $\Delta C_{D_{A_f}}$ to the drag of the standard fins used in Method B.

The fully appended torpedo drag, based on cross-sectional area is

$$(5)\quad C_{D_A} = C_{D_{A_{(\text{Method B})}}} + 0.31\, d/\ell\, C_{D_{S_R}} + C_{D_{A_{\text{parasite}}}} + C_{D_{A_c}} + \Delta C_{D_{A_f}}$$

or

$$(6)\quad C_{D_A} = C_{D_{A_{(\text{Method B})}}} + 0.31\, d/\ell\, C_{D_{S_R}} + C_{D_{A_{\text{parasite}}}} + C_{D_{A_c}} + \left[0.93\, c_{f_{\text{fins}}}(1.135 + 2t/c) + \frac{t}{b-a}(0.16\, t/c + 0.017) - 0.00024\,\frac{c}{b-a} + 0.00093\,(9.5 - \ell^*/d) \right] \frac{10.2c\,(b-a)}{d^2} - 0.0190 + 0.00122\,\ell^*/d$$

METHOD ILLUSTRATED WITH TORPEDO EX-2A

The drag of a full-scale Torpedo EX-2A was measured at DTMB[3] and a value of $C_{D_A} = 0.095$ obtained. Since the fin shape of this torpedo is approximately equal to that used in this study, and the water-tunnel model was smooth and without holes or gaps, Method B may be used to estimate the drag of the Torpedo EX-2A.

From a drawing of the torpedo

$$\ell^*_t/d = 3$$

$$\ell_{c_o}/d = 4.9$$

$$\ell_n/d = 0.5$$

$$d_n/d = 0.5$$

The test Reynolds number is

$$R_\ell = 3.18 \times 10^7$$

The nose correction factor from Fig. 6 is

$$\Delta\ell_c/d = -0.9$$

Therefore

$$\ell_c/d = 4.9 - 0.9 = 4.0$$

The drag coefficient found from Fig. 11 is

$$C_{D_A} = 0.100$$

The difference between this estimated value and the measured value is 5 percent.

---

[3] Informal Confidential letter from H. Eggers, David Taylor Model Basin, to S. Thurston, Naval Ordnance Test Station, dated 29 June 1954.

CONCLUSIONS

The methods described in this report may be used to determine the optimum torpedo configuration for a given application or to calculate the drag of a specific (existing) torpedo configuration. Specific conclusions regarding these methods and their application may be stated as follows:

1. The minimum drag per unit volume of a fully appended torpedo is obtained when the tail-cone fineness ratio is 6 or greater, irrespective of cylindrical section length. For smaller tail-cone fineness ratios, the drag is minimized when the cylindrical section is 6 or more diameters in length. These conclusions are based upon the study of a systematic series of torpedoes(called standard in this report) having a body fineness ratio between 2 and 13 and the volume-speed constant ($\forall^{1/3} V_o$) equal to 120. These qualitative conclusions are believed to be valid for other torpedoes which do not differ greatly from this size and speed.

2. Method A of this report can be used for quickly estimating the drag coefficient of any conventional torpedo configuration similar to the systematic series considered. It can be useful to the designer in approximating an optimum torpedo configuration.

3. Method B can be used for estimating the drag of any torpedo similar to the systematic series considered but of different volume and operating speed. The drag of most conventional torpedoes can be quickly calculated by use of this method.

4. Method C is used for estimating the drag of torpedoes with volume, velocity, fin size, and surface condition markedly different from the standard series considered in this report. Although this method is slightly longer than Methods A and B, it can be used for accurately estimating the drag of any torpedo dissimilar to the standard series.

5. It is assumed that the flow is fully turbulent and that no separation occurs at the nose. Empirical data are used in several sections of this report which introduce some error caused by the experimental scatter. It is believed that the methods shown here for estimating torpedo drag are sufficiently accurate for preliminary design purposes, but that more experimental data are needed to fully verify the conclusions and refine the empirical equations.

Appendix A

CALCULATION FOR DRAG OF CYLINDER SECTION

One method of calculating the drag of a body of revolution (Ref. 15) involves the step-by-step determination of the momentum thickness of the boundary layer, from the nose to the tail and into the wake beyond. The total drag is then proportional to the momentum area of the wake far downstream. This method can be modified to permit the calculation of the drag added by a cylindrical midsection by computing the change in the momentum area of the wake.

A simplified equation for the momentum thickness θ of a turbulent boundary layer, where θ is much smaller than the local body radius r_w, is (from Ref. 15)

$$(7)\quad \left(\frac{V}{V_o}\right)_e^{3.9732} \left(\frac{r_w\theta}{\ell^2}\right)_e^{1.1686} = \left(\frac{V}{V_o}\right)_b^{3.9732} \left(\frac{r_w\theta}{\ell^2}\right)_b^{1.1686}$$

$$+ \frac{(1.1686)(0.006361)}{(R_\ell)^{0.1686}} \int_{\ell_b/\ell}^{\ell_e/\ell} \left(\frac{r_w}{\ell}\right)^{1.1686} \left(\frac{V}{V_o}\right)^{3.8046} \sec\alpha \frac{d\ell}{\ell}$$

along the cylindrical section

(8)
$$r_{w_b} = r_{w_e} = \frac{d}{2}$$

and since the angle between the surface of the body and the longitudinal axis is 0 degrees

(9)
$$\sec \alpha = 1$$

For moderate pressure gradients it may be assumed that the velocity is the same at the beginning and end of the cylindrical midsection,

(10)
$$\left(\frac{V}{V_o}\right)_b = \left(\frac{V}{V_o}\right)_e$$

Thus for this particular case Eq. 7 can be simplified to

(11)
$$\theta_e^{1.1686} - \theta_b^{1.1686} = 0.001116 \frac{\ell}{\left(V_o\right)^{0.1686}\left(\frac{V_{e,b}}{V_o}\right)^{3.973}} \int_{\ell_b/\ell}^{\ell_e/\ell} \left(\frac{V}{V_o}\right)^{3.8046} \frac{d\ell}{\ell}$$

In order to solve for $\Delta\theta$, where

(12)
$$\Delta\theta = \theta_e - \theta_b,$$

an additional relationship between θ_e and θ_b is necessary. Since the exponents of θ_b and θ_e in Eq. 11 are close to unity, an

approximate equation will suffice. For a flat plate in turbulent flow, according to Ref. 18

(13) $$\theta = \text{constant} \times (R_\ell)^{-1/5}\ell$$

so that approximately

(14) $$\theta \propto \ell$$

Assuming this to be approximately true for the streamlined forebody and cylindrical section gives

(15) $$\frac{\theta_e}{\theta_b} = \frac{\ell_e}{\ell_b}$$

Equations 11 and 15 are solved simultaneously for $\Delta\theta$. The velocity distribution over the cylindrical section is estimated using the experimental results in Ref. 5, 19, and 20, and the integral is evaluated numerically. The increment of momentum area is

(16) $$\Delta\Omega = d/2\ \Delta\theta$$

Again using Ref. 15, the effect of the velocity distribution over the tail on the change in momentum area in the wake is

(17) $$\Delta\Omega_\infty = \left(\frac{V_e}{V_o}\right)^{3.4} \Delta\Omega$$

and finally the drag of the cylindrical section is

(18) $$D_C = 4\pi\Omega_\infty q_o$$

The drag coefficients for streamlined bodies with cylindrical midsections calculated by this method agree well with the limited test data that are available (Ref. 14).

Appendix B

CALCULATION FOR DRAG OF TAIL FINS

Two problems are involved in adding stabilizing fins to the series of torpedo bodies. First, for purposes of comparison it is necessary to add the proper-size fins to give equal stability to each body, and second, the added drag of the fins must be determined.

It has been shown[4] that the stability and controllability of widely different torpedo configurations is approximately the same if the tail-lift coefficients based on the frontal area of the torpedoes are equal.

A partly empirical, partly theoretical formula for the lift coefficient derivative of four cruciform fins placed on a body of revolution is developed in Ref. 21,

$$L'_{\beta_t} = 16 \frac{b^2}{d^2} \frac{(1 - a^2/b^2)}{\left(\sqrt{b^2/c^2 + 1} + 1\right)} \tag{19}$$

The fin and body dimensions a, b, c, and d are defined in Fig. 13. For this study a value of $L'_{\beta_t} = 1.8$ is chosen, which

[4] In a report on stability of torpedoes, by L. Lopes, D. Elliott, and others, in preparation at this Station.

results in an average torpedo dynamic stability. An average torpedo-fin configuration is used composed of four cruciform fins, each pair having an over-all aspect ratio of 3 $\left(AR = 3 = \frac{2b}{c}\right)$. These fins are placed on the torpedo body at a point where the fin midpoint lies at an effective diameter of one half the maximum diameter (a/b = 1/2). Thus, the fin-tip radius, b, is 0.62d and the chord length, c, is 0.414d.

The drag of the fins is found by adding the skin-friction drag and the additional drag caused by body-fin interference. These drags are expressed as drag coefficients based on fin surface area and are estimated, using Ref. 6 and other sources, as follows:

1. The fin-skin-friction drag including the overvelocity effect is

$$\left(C_{D_{S_f}}\right)_{friction} = C_f\,(1 + 2\,t/c) \tag{20}$$

2. The form drag of the fins (Ref. 16) is

$$\left(C_{D_{S_f}}\right)_{form} = C_f\left[60\,(t/c)^4\right] \tag{21}$$

or for small t/c

$$\left(C_{D_{S_f}}\right)_{form} \cong 0 \tag{22}$$

3. The correction for the momentum thickness of the boundary layer is applied by reducing the fin-surface area by the amount

covered by the torpedo-body momentum thickness θ. The fin drag is defined as

$$D_{f_o} = C_{D_{S_f}} q_o S_f$$

The reference surface area S_f for four fins is defined as

(23) $$S_f = 8c(b - r - \theta) = 8c(b - a)$$

where r is the body radius at the fin midchord.

An approximate expression for θ is

(24) $$\theta \cong 0.0025\, \ell^*$$

A more exact value obtained from Ref. 21 is

$$\theta \cong \left(\frac{d}{2r}\right) 0.022 \ell_{\text{leading edge}} R\ell^{-1/6}_{\text{leading edge}}$$

4. The interference drag caused by the effect of the fins on the pressure distribution of the body (Ref. 16) is

(25) $$\left(C_{D_{S_f}}\right)_{\text{body pressure}} = 1.6 \frac{(\Delta q/q_o)}{\Delta \ell/\ell} C_{D_S}$$

$$\cong 1.6 \frac{\left(\frac{q_{\text{leading edge}}}{q_o} - 0.87\right)^2}{\left(1 - \frac{\ell_{\text{leading edge}}}{\ell}\right)} \left(C_{D_{S_f}}\right)_{\text{friction}}$$

5. The interference drag caused by the effect of the body on the pressure distribution of one fin (Ref. 16) is

$$(26)\quad \left(C_{D_{S_f}}\right)_{\text{fin pressure}} = \left[0.8\ t/c\left(t/c + 0.25\,\frac{\Delta p}{q_o}\right)^2 - 0.0005\right]\frac{c^2}{S_f}$$

or, for four fins where S_f is $8c(b - a)$,

$$(27)\quad \left(C_{D_{S_f}}\right)_{\text{fin pressure}} = 0.4\left(\frac{t}{b - a}\right)\left(t/c + 0.25\,\frac{\Delta p}{q_o}\right)^2 - 0.00025\left(\frac{c}{b - a}\right)$$

6. Because the dynamic pressure over the tail cone is lower than the free-stream dynamic pressure, the estimated total drag of the fins must be multiplied by the local dynamic pressure ratio

$$(28)\quad D_f = D_{f_o}\ q/q_o$$

7. The drag of holes and rudder gaps, if any, is estimated by the methods of Ref. 16.

8. The thickness of the boundary layer over the tail cone modifies No. 4 and 5 above by submerging the fins and increasing or decreasing the effect of the pressure interference. To estimate the magnitude of this correction, all of the available data (Ref. 8, 9, 22 - 26) were used in which both bodies and bodies with fins were tested. To the measured bare-body drag was added the sum

of the drags estimated, using Eq. 20 - 28. The difference between this estimated fin drag and the measured fin drag is $\Delta_{C_{D_{S_f}}}$, the empirical boundary-layer interference drag shown in Fig. 9. Although there is considerable scatter in the data because of the inaccuracy inherent in taking a small difference of two large drag measurements, the generally decreasing trend of the fin drag as the boundary layer thickens is apparent. Thus, as ℓ/d increases, the momentum thickness increases, and the added drag from pressure interference in the intersection between the body and fins decreases, finally becoming less than that predicted by corrections No. 4 and 5 above and making $\Delta C_{D_{S_f}}$ negative. The equation for this correction is

$$\Delta C_{D_{S_f}} = 0.001\ (9.5 - \ell^*/d) \tag{29}$$

The total drag of the fins, using the corrections given by Eq. 20 - 29 and Fig. 9, is then

$$C_{D_{S_f}} = \frac{\text{Fin drag}}{q_o\ S_f} \tag{30}$$

$$= q/q_o \left\{ C_f \left[1 + 2\ t/c + 1.6 \frac{\left(\frac{q_{\text{leading edge}}}{q_o} - 0.87 \right)^2}{\left(1 - \frac{\ell_{\text{leading edge}}}{\ell} \right)} \right] + 0.4 \frac{t}{b-a} \left(\frac{t}{c} + 0.25 \frac{\Delta p}{q} \right)^2 - 0.00025 \frac{c}{b-a} + 0.001\ (9.5 - \ell^*/d) \right\}$$

For the case of four fins mounted on the tail cone, it can be assumed that $\frac{q_{\text{leading edge}}}{q_o} \cong 1$, $\frac{\ell_{\text{leading edge}}}{\ell} \cong 0.8$, $\frac{\Delta p}{q} \cong 0.87$ and $\frac{q}{q_o} = 0.93$.

Then, neglecting higher order terms in t/c,

$$(31)\quad C_{D_{S_f}} \cong 0.93\, C_{f_{fin}}(1.135 + 2\ t/c) + \frac{t}{b - a}(0.16\ t/c + 0.017) - 0.00024\,\frac{c}{b - a} + 0.00093(9.5 - \ell^*/d)$$

In estimating the drag of the fins to be added to the series of bodies, it was assumed that the thickness-to-chord ratio of the fins is 0.05. It was also assumed that the drag of gaps and holes is negligibly small, and the fin sizes were as described in the first part of this Appendix.

The total drag of the fins is then

$$(32)\quad C_{D_{S_f}} = 1.15\, C_{f_{fins}} + 0.0102 - 0.00093\,\ell^*/d$$

In estimating the drag of a torpedo by Methods A or B of this report, it is assumed that the fin drag is given by Eq. 32. A more accurate procedure for finding the drag of torpedoes with widely different tail configurations is given by Method C. The difference in the fin-drag coefficient from the standard fin size assumed in Eq. 32 and an arbitrary fin is obtained by subtracting Eq. 31 from Eq. 32. Making the simplifying assumption that $C_{f_{fin}}$ in Eq. 32 $\cong 0.0037$, the difference in the fin-drag coefficient based on cross-sectional area of the torpedo is

$$(33)\quad \Delta C_{D_{A_f}} = \left[0.93\, C_{f_{fin}}(1.135 + 2\ t/c) + \frac{t}{b-a}(0.16\ t/c + 0.017)\right.$$

$$\left. - 0.00024\frac{c}{b-a} + 0.00093(9.5 - \ell^*/d)\right]\frac{10.2c(b-a)}{d^2}$$

$$- 0.0190 + 0.00122\,\ell^*/d$$

where the ratio of fin surface area to torpedo cross-section area is

$$\frac{S_f}{A} = \frac{8c(b-a)}{\pi/4\ d^2} = 10.2c\ \frac{(b-a)}{d^2}$$

For the standard fin, $\left(\frac{S_f}{A}\right)_{standard} = (10.2)\ (0.414)\ (0.31) = 1.31$

NOMENCLATURE

A Cross-section area of torpedo, sq ft

a, b, c Fin dimensions shown in Fig. 13, ft

C_f Skin-friction drag coefficient

$$C_f = \frac{\text{skin-friction drag (lb)}}{q_o S}$$

C_{D_S} Total drag coefficient based on surface area

$$C_{D_S} = \frac{\text{total drag (lb)}}{q_o S}$$

$C_{D_{S_f}}$ Fin drag coefficient based on fin surface area

$$C_{D_{S_f}} = \frac{\text{fin drag (lb)}}{q_o S_f}$$

C_{D_A} Total drag coefficient based on cross-section area

$$C_{D_A} = \frac{\text{total drag (lb)}}{q_o A}$$

$C_{D_{A_{parasite}}}$ Parasite drag coefficient based on cross-section area

$$C_{D_{A_{parasite}}} = \frac{\text{parasite drag (lb)}}{q_o A}$$

$C_{D_{A_R}}$ Roughness drag coefficient based on cross-section area

$C_{D_\forall}$ Total drag coefficient based on volume

$$C_{D_\forall} = \frac{\text{total drag (lb)}}{q_o(\forall)^{2/3}}$$

$C_{D_{A_c}}$ Drag coefficient from truncated tail cone, based on cross-section area

C_p Prismatic coefficient

$$C_p = \frac{\forall}{\pi/4\ d^2}$$

C_r Residual or form drag coefficient based on surface area,

$$C_r = \frac{\text{residual drag (lb)}}{q_o S}$$

d Maximum diameter of torpedo, ft

d_B Diameter of truncation on tail cone, ft

D Drag, lb

D_f Fin drag, lb

D_R Roughness drag, lb

$\Delta C_{D_{S_f}}$ Added drag coefficient of fins caused by boundary-layer interference Fig. 14

$$\Delta C_{D_{S_f}} = \frac{\text{added drag due to boundary layer interference (lb)}}{q_o S_{fins}}$$

$C_{D_{S_R}}$ Added drag coefficient of torpedo from holes and roughness

$$\Delta C_{D_{S_R}} = \frac{\text{added drag due to roughness and holes (lb)}}{q_o S}$$

L'_{β_t} Tail lift coefficient based on cross-section area

$$L'_{\beta_t} = \frac{\text{tail lift (lb)}}{q_o A \beta}$$

ℓ^*_t Length of the torpedo tail cone, measured to the extended tip, ft

ℓ Torpedo length, ft

ℓ^* Torpedo length, measured to the extended tail cone tip, ft

ℓ/d Body fineness ratio

$\frac{\Delta \ell_c}{d}$ Nose-shape correction factor (from Fig.6)

m Ratio of the position of maximum thickness from nose to the over-all length of streamlined body

$\Delta p/q_o$ Change in the static pressure ratio on a body

$\Delta q/q_o$ Change in the dynamic pressure ratio on a body along the chord length of the fins

q Dynamic pressure, lb/sq ft

$$q = 1/2\ \rho V^2$$

q_o Free-stream dynamic pressure, lb/sq ft

$$q_o = 1/2\ \rho V_o^2$$

R_ℓ Reynolds number based on over-all length

$$R_\ell = \frac{V_o \ell}{\upsilon}$$

r Local radius of the body at the fin midchord, ft

r_w Local radius of the body, ft

S Surface area, ft^2

t Thickness of a fin, ft

$\forall$ Torpedo body volume, ft^3

V Local velocity, ft/sec

V_o Free-stream velocity, ft/sec

α Angle between tangent to surface and axis of the body

β Angle of attack of the body (radians)

δ Thickness of the boundary layer, ft

θ Momentum thickness of the boundary layer, ft

$$\theta = \int_0^{\delta} \left(1 - \frac{V}{V_o}\right) \frac{V}{V_o} \, d\delta$$

Ω Momentum area of the boundary layer, ft^2

$$\Omega = \int_0^{\delta} \left(1 - \frac{V}{V_o}\right) \frac{V}{V_o} \, r_w d\delta$$

υ Kinematic viscosity of the fluid, ft^2/sec

SUBSCRIPTS

b The longitudinal station located at the forward end of the cylindrical midsection

c The cylindrical midsection

e The longitudinal station at the after end of the cylindrical midsection

F The forebody of a streamlined shape such as the DTMB Series 58

N Any arbitrary nose shape

O Drag coefficients, Reynolds numbers, etc., of a specific configuration

T The tail section of a streamlined shape such as the DTMB Series 58

REFERENCES

1. Aeronautical Research Committee. Tests on Two Streamline Bodies in the Compressed Air Tunnel, by D. H. Williams, R. Jones, and A. F. Brown. London, ARC, 1936. (ARC R. and M. No. 1710.)

2. David Taylor Model Basin. .... Washington, DTMB, April 1950. (DTMB Report C-297), CONFIDENTIAL.

3. ------. .... Washington, DTMB, 1951. (DTMB Report C-343), CONFIDENTIAL.

4. ------. .... Washington, DTMB, 1951. (DTMB Report C-343), CONFIDENTIAL.

5. Aeronautical Research Committee. The Calculation of the Total and Skin Friction Drags of Bodies of Revolution at Zero Incidence, by A. D. Young. London, ARC, 1944. (ARC R. and M. No. 1874.)

6. National Advisory Committee for Aeronautics. Force Measurements on a 1/40 Scale Model of the U. S. Airship "Akron," by H. B. Freeman. Washington, NACA, 1932. (NACA Report 432.)

7. ------. Drag of C-Class Airship Hulls of Various Fineness Ratios, by A. F. Zahm, R. H. Smith, and F. A. Louden. Washington, NACA, 1928. (NACA Report 291.)

8. Zeppelin Airship Works. Aerodynamic Model Tests With German and Foreign Airship Designs in the Wind Tunnel of the Zeppelin Airship Works, by M. Schirmer. Friedrichshafen, ZWB, April 1942. (ZWB Report F. B. 1647.)

9. Stevens Institute of Technology, Experimental Towing Tank. .... Hoboken, N. J., SIT, December 1948. (SIT ETT Report 356), CONFIDENTIAL.

10. National Advisory Committee for Aeronautics. .... Washington, NACA, 1950. (NACA RM SL50E09a), CONFIDENTIAL.

11. Stevens Institute of Technology, Experimental Towing Tank. .... Hoboken, N.J.,SIT, 1955. (SIT ETT Report 547), CONFIDENTIAL.

12. National Advisory Committee for Aeronautics. Tests of the NPL Airship Models in the Variable Density Wind Tunnel, by G. Higgins. Washington, NACA, 1927. (NACA TN 264.)

13. ------. Airship Model Tests in the Variable Density Wind Tunnel, by I. Abbot. Washington, NACA, 1931. (NACA 394.)

14. David Taylor Model Basin. .... Washington, DTMB, (DTMB Report C-738), CONFIDENTIAL.

15. ------. The Calculation of the Viscous Drag of Bodies of Revolution, by P. Granville. Washington, DTMB, July 1953. (DTMB Report 849.)

16. Hoerner, S. F. Aerodynamic Drag. Midland Park, N.J., 1951. (Published by author.)

17. U. S. Naval Ordnance Test Station. Effect of Torpedo Paint Roughness on Torpedo Speed, by J. D. Brooks. Pasadena, Calif., NOTS, 9 February 1956. (Memorandum No. GC 641.)

18. Schlichting, H. Boundary Layer Theory. New York, McGraw-Hill, 1955. P. 433.

19. Iowa Institute of Hydraulic Research. Cavitation and Pressure Distribution, Head Forms at Zero Angle of Yaw, by H. Rouse and J. S. McNown. Iowa City, Iowa, IIHR, 1948. (Bulletin 32.)

20. David Taylor Model Basin. .... Washington, DTMB, May 1950, (DTMB Report C-314), CONFIDENTIAL.

21. U. S. Naval Ordnance Test Station. The Stability Coefficients of Standard Torpedoes, by M. R. Bottaccini. China Lake, Calif., 18 July 1954. (NAVORD Report 3346, NOTS 909.)

22. ------. Wind Tunnel Tests on an Unpowered Model of a Research Torpedo Configuration, by F. J. Hill, Jr. China Lake, Calif., NOTS, 11 February 1957. (NAVORD Report 5428, NOTS 1691.)

23. David Taylor Model Basin. .... Washington, DTMB, (DTMB NRS 724), CONFIDENTIAL.

24. ------. .... Washington, DTMB, September 1952. (DTMB Report C-526), CONFIDENTIAL.

25. Stevens Institute of Technology, Experimental Towing Tank. .... Hoboken, N.J.,SIT, January 1949. (SIT ETT Report 357), CONFIDENTIAL.

26. ------. .... Hoboken, N.J.,SIT, November 1949. (SIT ETT Report 387), CONFIDENTIAL.

INITIAL DISTRIBUTION

3 Chief, Bureau of Ordnance
    Ad3 (1)
    ReU (1)
    ReU1 (1)
1 Chief, Bureau of Aeronautics
1 Chief, Bureau of Ships (Code 560)
1 Chief of Naval Operations
1 Chief of Naval Research (Code 466)
1 David W. Taylor Model Basin
1 Naval Advanced Undersea Weapons School, Key West
1 Naval Aircraft Torpedo Unit, Naval Air Station, Quonset Point
3 Naval Gun Factory (Code 752)
1 Naval Ordnance Laboratory, White Oak
1 Naval Ordnance Unit, Key West
1 Naval Postgraduate School, Monterey (Technical Reports Section)
1 Naval Proving Ground, Dahlgren (Code Ad)
2 Naval Records Management Center, Alexandria
1 Naval Research Laboratory
1 Naval Torpedo Station, Keyport
1 Naval Underwater Ordnance Station, Newport
5 Armed Services Technical Information Agency (TIPDR)
1 National Advisory Committee for Aeronautics
1 Aerojet-General Corporation, Azusa, Calif., via BAR
1 Applied Physics Laboratory, University of Washington, Seattle
1 Bendix Aviation Corporation, Pacific Division, North Hollywood
1 Brush Electronics Company, Cleveland
1 Clevite Research Center, Cleveland
1 CONVAIR Scientific Research Laboratory, San Diego (A. L. Berlad)
1 Electric Boat Division, General Dynamics Corporation, Groton, Conn. (Carlton Shugg)
1 Experimental Towing Tank, Stevens Institute of Technology, Hoboken, N. J.
1 Fairchild Engine and Airplane Corporation, Fairchild Engine Division, Deer Park, N. Y.
1 General Electric Company, Missiles and Ordnance Systems Department, Pittsfield, Mass. (Underwater Ordnance Sales)
1 Hydrodynamics Laboratory, CIT, Pasadena (Executive Committee)
1 Ordnance Research Laboratory, Pennsylvania State University (Development Contract Administrator)

1 Propulsion Research Corporation, Santa Monica, Calif. (Engineering Librarian)
1 Vitro Corporation of America, Silver Spring
1 Westinghouse Electric Corporation, Baltimore (Engineering Librarian)
1 Westinghouse Research Laboratories, Pittsburgh (Arthur Nelkin)
1 Woods Hole Oceanographic Institute, Woods Hole, Mass.

NAVY NOTS AND CHINA LAKE, CALIF., 1331 6/58 125